Phase Diagrams of Nanometer-Sized Particles in Binary Systems

Junggoo Lee, Joonho Lee, Toshihiro Tanaka, Hirotaro Mori, and Karri Penttilä

A study on alloy phase formation in nanometer-sized particles by in-situ transmission-electron microscopy revealed that the phase equilibrium of these particles is significantly different from that of the corresponding bulk materials. A theoretical study was conducted based on thermodynamics modified so that Gibbs free energies for bulk materials available in the CALPHAD database were modified by taking into consideration factors affecting the phase equilibrium of nanometer-sized alloy particles. The study proved useful to evaluate the results obtained from experiments.

INTRODUCTION

It is now well established that nanometer-sized materials exhibit electronic, magnetic, optic, and thermal properties that are significantly different from those of the corresponding bulk materials.[1,2] How to create new properties by manipulating materials in the nanometer range is a scientific and technological challenge. In addition, there is an urgent need for the phase diagram of nanometer-sized alloy systems to extend the usage of new functional nanometer-sized particles in such fields as nanoelectronics and catalysis.

There are actually several reports on the phase diagram of nanometer-sized alloy systems, but most of them are based on only theoretical calculations.[3,4] Experimental studies on nanometer-sized (especially isolated) alloy particles are, on the other hand, quite limited. The limitation comes from the fact that it was in the past rather difficult to control and measure such parameters as temperature (T), size (d), and composition (C) at the same time in one isolated nanometer-sized alloy particle. Recent remarkable progress in transmission-electron microscopy (TEM), however, makes it possible to examine the phase stability of an isolated nanometer-sized particle as a function of temperature, size, and composition.[5–8]

The use of thermodynamic calculations based on the CALPHAD (Calculation of Phase Diagram) method can be extended from bulk to nanometer-sized systems if one takes the finite size effect into consideration in the calculation. This is a useful approach for constructing the phase diagram of nanometer-sized alloy particles.

This article describes the use of in-situ TEM to examine the phase equilibrium of an isolated nanometer-sized alloy particle. The experimental results were also compared with results obtained from thermodynamic calculations in which factors affecting the phase equilibrium of nanometer-sized alloy particles were taken into consideration. In addition, recommendations for the future studies are given.

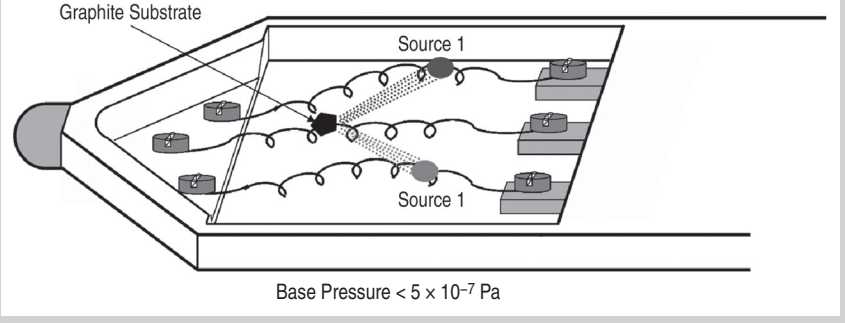

Figure 1. A schematic illustration of a side-entry holder equipped with a unique double-source evaporator.

IN-SITU TEM OBSERVATION OF ALLOY PHASE FORMATION

Much work on the characterization of nanometer-sized particles, especially on the microstructural (or phase) analysis, has been carried out using TEM. However, most of properties of nanometer-sized particles are very sensitive to the surface cleanliness; therefore the surface of nanometer-sized particles must be kept as clean as possible during the experiments. For this reason, the authors developed in-situ experiments with TEM in which both production and observation of nanometer-sized particles are possible in the same vacuum chamber without exposing particles to any undesired atmosphere. This technique uses a unique side-entry TEM holder equipped with a double-source evaporator, which is an improved version of a hot holder designed by Kamino and Saka.[9] A schematic illustration of the holder used is shown in Figure 1. The essential part of the holder consists of three spiral-shaped tungsten filaments. The middle filament was attached with a flake of graphite (other materials can also be used) used as the supporting

substrate, and the outer two filaments were attached with source materials. Prior to experiments, the graphite flake was baked at 1,070 K for 60 s by feeding an appropriate amount of current on the middle filament. After being baked, the graphite substrate was cooled down to a desired temperature (T1). After that, one source material was evaporated from the second filament onto the graphite substrate kept at T1, and nanometer-sized pure particles were produced on the substrate. The other source material was then evaporated from the third filament onto the nanometer-sized pure particles, keeping the temperature of the substrate at T1. Microstructural changes in an isolated particle associated with alloying of solute atoms were studied in-situ in the microscope using a supersensitive television camera (GATAN 622SC) with a time resolution of 30 frames s^{-1}. Images obtained were recorded on videotapes through a video recorder system connected to the television camera. A 200 kV Hitachi HF-2000 high-resolution electron microscope (HREM), which was equipped with a field emission gun, was employed. The chemical composition of an isolated nanometer-sized alloy particle was examined with energy-dispersive x-ray spectroscopy (EDS). The base pressure in the microscope was less than 5×10^{-7} Pa.

DEPRESSION OF THE EUTECTIC POINT

Figure 2 shows a typical sequence of the alloying process of tin atoms into nanometer-sized bismuth particles at around 350 K. The three numbers inserted in each micrograph indicate the time in units of minutes, seconds, and one-sixtieth seconds. Figure 2a shows an as-produced pure bismuth particle. The size of the particle was approximately 8 nm. The $(01\bar{1}2)$ lattice fringes of pure bismuth and the (0001) lattice fringes of graphite substrate are clearly shown. Figure 2b shows the same particle after tin deposition. With the deposition of tin atoms, the structure of the particle changed from a single crystal to a mixture of a crystalline phase and a liquid phase. The liquid phase corresponds to the portion in uniform contrast in the upper right part of the particle (Figure 2b). A faceted surface of the crystalline bismuth (shown in Figure 2a) was replaced by a round, curved surface of the liquid phase (arrowed).

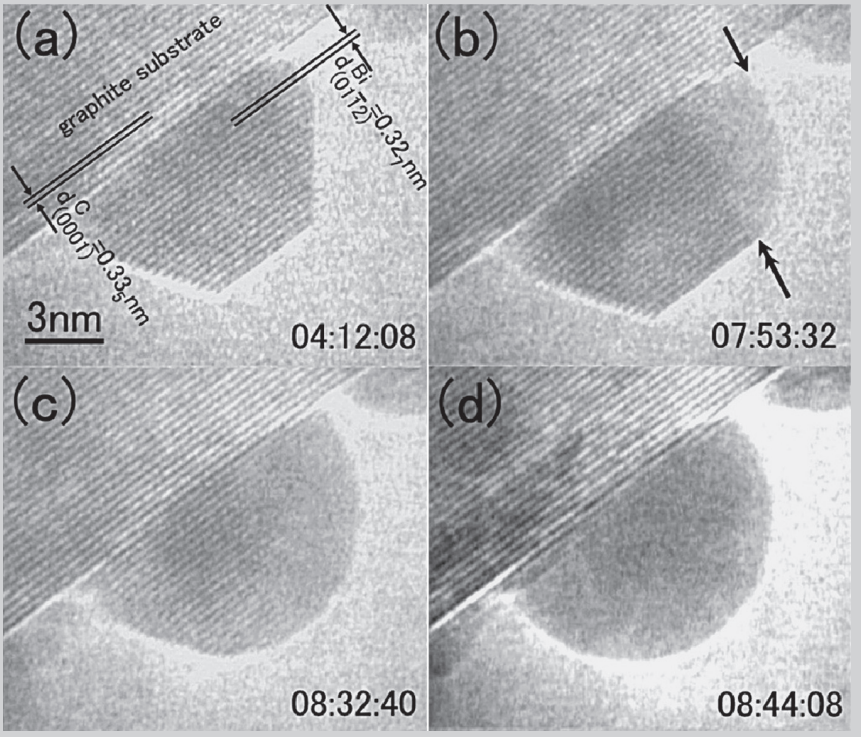

Figure 2. A sequence of the alloying process of tin atoms into a nanometer-sized bismuth particle. (a) An as-produced bismuth particle on the graphite substrate. In (b) through (d), the same particle is shown under a tin deposition condition. With tin deposition, a crystalline/liquid interface was first formed in the particle (double-arrowed in (b)) and it then moved left and downward at the expense of crystal (see (c)) until the whole particle became liquid (see (d)).[7]

With continued deposition of tin atoms, the crystal/liquid interface moved left and downward at the expense of crystal (Figure 2c), and eventually the whole particle became liquid (Figure 1d). An EDS spectrum taken from the central portion of the particle in Figure 2d showed that the composition of the particle was Bi-50 at.% Sn (not shown here). It took about 4.5 min. to form the liquid alloy particle (Figure 2d) by alloying tin atoms into the pure bismuth particle (Figure 1a). This period can be considered to be long enough for the alloy particle to maintain its equilibrium state. The described change in microstructure (i.e., crystalline→(crystalline+liquid)→liquid) is consistent with that predicted from the phase diagram for the bulk materials at temperatures between the eutectic point (Teu, 412 K) and the melting point of bismuth. But this phase change was observed approximately 60 degrees below the eutectic point of the corresponding bulk alloy, as shown in Figure 2. This result provides direct evidence for the fact that due to the finite size effect, the eutectic point of the system is suppressed to a temperature below 350 K.

A phenomenon similar to the eutectic point suppression has been observed in other binary systems. For example, when the size of particles is smaller than approximately 10 nm in diameter, a thermodynamically stable amorphous phase and liquid phase were formed at room temperature (RT) in alloy particles over a compositional range near the eutectic composition in the Au-Sn and In-Sn systems,[10,5] respectively. Here, "thermodynamically stable amorphous phase" refers to the observation that, upon heating, it went to melt without crystallization and, upon cooling, it solidified into an amorphous solid with no traces of crystallization. The observation suggests the Gibbs free energy of the amorphous phase should be lower than that of a crystalline counterpart(s) at least at temperatures near and above room temperature where observations were carried out. It should be noted here that both the amorphous phase in

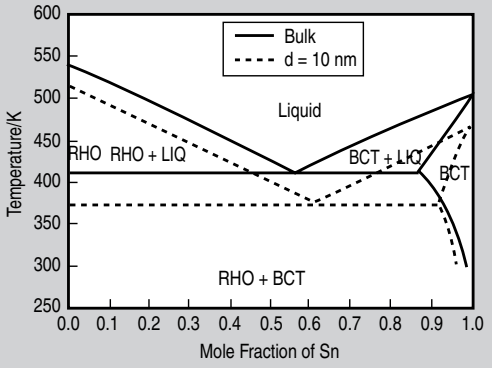

Figure 3. A phase diagram of the Sn-Bi system in which (a) the bulk phase is shown with a solid line and (b) the nano phase is shown with a dashed line (d = 10 nm).

the former system and the liquid phase in the latter system cannot be present at RT as phases more stable than crystalline counterparts in bulk materials. The formation of the thermodynamically stable amorphous and the liquid phase is ascribed to the enhanced suppression of Teu with size reduction.

When the three temperatures—Teu, glass transition (Tg), and RT (where the observation is carried out)— are ordered as Tg>RT>Teu in nanometer-sized particles in the Au-Sn system, due to the enhanced suppression of Teu it is postulated that a crystalline-to-amorphous (C→A) phase change would be induced by simply adding solute atoms (i.e., tin atoms) onto nanometer-sized crystalline particles of pure gold at RT. This postulation is in agreement with what is observed by experiment.[10] When Teu, Tg, and RT lie in such an order as RT>Tg>Teu in nanometer-sized particles in the In-Sn system, it is postulated that a crystalline-to-liquid (C→L) phase transition would be induced by simply adding solute atoms (i.e., In atoms) onto nanometer-sized crystalline particles of pure tin at RT. This postulation is again in agreement with what is observed experimentally.[5] When the temperatures Teu, Tg, and 350 K (where the observation is carried out) are ordered as 350 K>Tg>Teu in nanometer-sized particles in the Sn-Bi system,[6] it is then postulated that at 350 K a sequential change of crystalline→(crystalline + liquid)→liquid would be induced by simply adding solute atoms (i.e., tin atoms) onto nanometer-sized crystalline particles of pure bismuth. This postulation is in agreement with what is observed by experiments as shown in Figure 2.

Based upon these results, it seems that although different types of phase changes are observed in particular systems (i.e., C→A in the Au-Sn system, C→L in the In-Sn system, and C→(C+L)→L in the Sn-Bi system), all the behaviors are explained in terms of the relative position among Tg and Teu in the systems, and the temperature at which experiments were performed (i.e., RT and 350 K). The relative position is essentially determined by the magnitude of Teu suppression with decreasing particle size.

THEORETICAL ASSESSMENT

Since the effect of free surface on the total thermodynamic properties cannot be ignored in nanometer-sized particles because of the large surface-to-volume ratio, the phase relations are dependent upon the size of the particle and its surface property. The authors have established a thermodynamic model to evaluate the phase diagrams of binary system as a function of temperature, composition, and size.[11,12]

When a pure solid phase is selected as the reference state of Gibbs energy, the total Gibbs energies in liquid and solid phases, $\Delta G^{Total,Phase}$ (Phase = Liq., Sol.1, Sol.2, etc.), of a small particle with its radius r in an A-B binary system can be described in Equation 1. All equations are shown in Table I.

The Gibbs energies of the bulk of an A-B binary alloy in liquid and solid phases, $\Delta G^{Bulk,Phase}$, which correspond to $\Delta G^{Total,Phase}$ with $r = \infty$, are expressed in Equation 2, where $\Delta G_i^{Sol.\rightarrow Phase}$ (i = A or B) is the Gibbs energy of a pure component in each phase relative to the pure solid i. $G^{Excess,Phase}$ is the excess Gibbs energy of each phase in the A-B alloy, X_i is the mole fraction of a component i, R is the gas constant, and T is the temperature.The Gibbs energy of the surface, $\Delta G^{Surface,Phase}$ in Equation 1, is assumed as shown in Equation 3, where r is the radius of a particle (= 0.5 d), σ^{Phase} is the surface tension of each phase, V^{Phase} is the molar volume of each phase, $\sigma_i^{Sol.}$ is the surface tension of pure solid i, and $V_i^{Sol.}$ is the molar volume of pure solid i.

As an example, in the following section, the phase diagram of a 10 nm sized alloy particle of the Bi-Sn system was calculated by employing the theoretical model described and compared with that confirmed by experiment.

Table I. Equations

$$\Delta G^{Total,Phase} = \Delta G^{Bulk,Phase} + \Delta G^{Surface,Phase} \quad (1)$$

$$\Delta G^{Bulk,Phase} = N_A \Delta G_A^{Sol.\rightarrow Phase} + N_B \Delta G_B^{Sol.\rightarrow Phase} + G^{Excess,Phase} + RT(X_A \ln X_A + X_B \ln X_B) \quad (2)$$

$$\Delta G^{Surface,Phase} = \frac{2\sigma^{Phase} V^{Phase}}{r} - \frac{2(X_A \sigma_A^{Sol.} V_A^{Sol.} + X_B \sigma_B^{Sol.} V_B^{Sol.})}{r} \quad (3)$$

$$V^{Phase} = X_{Bi} V_{Bi}^{Phase} + X_{Sn} V_{Sn}^{Phase} \quad (4)$$

$$\sigma^{Phase} = \sigma_{Bi}^{Phase} + \frac{RT}{A_{Bi}} \ln \frac{X_{Bi}^{Surface}}{X_{Bi}^{Bulk}} + \frac{1}{A_{Bi}} G_{Bi}^{Excess,Phase,Surface} - \frac{1}{A_{Bi}} G_{Bi}^{Excess,Phase,Bulk} \quad (5)$$

$$\sigma^{Phase} = \sigma_{Sn}^{Phase} + \frac{RT}{A_{Sn}} \ln \frac{X_{Sn}^{Surface}}{X_{Sn}^{Bulk}} + \frac{1}{A_{Sn}} G_{Sn}^{Excess,Phase,Surface} - \frac{1}{A_{Sn}} G_{Sn}^{Excess,Phase,Bulk} \quad (6)$$

$$G_i^{Excess,Phase,Surface}(T, N_i^{Surface}) = 0.83 \cdot G_i^{Excess,Phase,Bulk}(T, N_i^{Surface}) \quad (7)$$

NANO PHASE DIAGRAM OF SN-BI BINARY SYSTEM

The Gibbs energies of the bulk liquid and solid phases (rhombohedral(Bi), body-centered tetragonal(Sn)) are obtained from Reference 13. Surface tensions of pure liquid metals were investigated within errors of ±1% by the authors.[14–17] It is assumed that the surface tension of pure solid metals at melting temperature is 25% larger than that of pure liquid metals, and that the temperature dependence is the same as that of pure liquid metals. The effect of crystal faces has been ignored. The molar volumes of pure metals are also available in the literature.[18] The molar volume of each phase was assumed as shown in Equation 4. The surface tension of a liquid and solid alloy, σ^{Phase}, is evaluated from the Butler's equation in Equations 5 and 6,[19] where $X_i^{Surface}$ and X_i^{Bulk} are the mole fraction of component i on the surface and the bulk, respectively. $A_i = 1.091 N_{Av.}^{1/3} (V_i^{Phase})^{2/3}$ ($N_{Av.}$ is the Avogadro number) is the molar surface area of pure i. For the excess Gibbs energy in the surface, Equation 7 was derived from the model proposed by Yeum et al.[20] The value of 0.83 is the ratio of the coordination number in the surface to that in the bulk considering the surface relaxation.[21–27] It has been confirmed that Equations 5–7 are suitable to estimate the surface tension of alloy systems.[15,16,20,24]

Figure 3 shows the calculated phase diagram of the Sn-Bi binary system, comparing phase diagrams of bulk and 10 nm-sized particles. The liquidus temperature of nanometer-sized particles decreased by ~50 K from that of bulk. The liquidus temperature of Sn-50at.%Bi is 405 K, which is slightly higher than that employed in the experiment (350 K), as shown in Figure 2. It is considered that the temperature difference is mainly due to the size difference between calculations and measurements. As the particle size decreases, the liquidus temperature decreases much more. Thus, it is considered that the calculation results are in accordance with the measurements.

FUTURE WORK

Effect of Substrates

The melting of nanometer-sized particles has been primarily investigated on solid substrates, so that interface tension, as well as surface tension, might also affect the melting temperature of nanometer-sized particles. However, the effect of substrates on the melting temperature was not taken into account explicitly in previous studies. Recently, the authors have pointed out that substrates might have some effect on the melting temperature of nanometer-sized particles.

Evaluation of Solid-Liquid Interfacial Tension

Previous studies revealed that the interfacial tension for an interface between liquid (or solid) and solid phases can affect the phase equilibrium when the particle is in the two-phase region (liquid-solid or solid-solid).[5–8] A model to evaluate the effect of interfacial tension on the phase equilibrium of nanometer-sized alloy particles is under construction.

Evaluation of Change in Surface Tension

Surface tension of small particles may change due to curvature, which may decrease with decreasing size, yielding a liquidus temperature drop. For pure gold, this effect would occur for the particles less than 10 nm.[17] Accordingly, an assessment of the phase diagram of particles less than 10 nm should consider the effects of this surface tension drop.

Glass Transition

As mentioned previously, a thermodynamically stable amorphous phase could be formed in a eutectic system when the size of particles is smaller than approximately 10 nm in diameter. This unique amorphous phase offers an opportunity for an in-depth understanding of the liquid-to-glass transition, an unsolved issue in modern solid-state physics.

ACKNOWLEDGEMENTS

This work was supported by "Priority Assistance of the Formation of Worldwide Renowned Centers of Research—The 21st Century COE Program (Project: Center of Excellence for Advanced Structural and Functional Materials Design)" and a grant-in-aid for scientific research from the Ministry of Education, Sports, Culture, Science and Technology of Japan (Grant No. 15074213 and 15206070). This work was partially supported by "Modelling of materials and surface properties in nanotechnology."

References

1. R.P. Andres et al., *J. Mater. Res.*, 4 (1987), p. 704.
2. W.P. Halperin, *Rev. Modern Phys.,* 58 (1986), p. 533.
3. M. Wautelet, J.P. Dauchot, and M. Hecq, *Nanotechnology*, 11 (2002), p. 6.
4. A.S. Shirinyan and A.M. Gusak, *Phil. Mag.*, 21 (2004), p. 579.
5. J.-G. Lee, H. Mori, and H. Yasuda, *Phys. Rev. B*, 65 (2002), p. 132106.
6. J.-G. Lee, H. Mori, and H. Yasuda, *Phys. Rev. B*, 66 (2002), p. 012105.
7. J.-G. Lee and H. Mori, *MPMD Fifth Global Innovations Proceedings on Surfaces and Interfaces in Nanostructured Materials and Trends in LIGA, Miniaturization, and Nanoscale Materials*, ed. S.M. Mukhopadhyay et al. (Warrendale, PA: TMS, 2004), p. 3.
8. J.-G. Lee and H. Mori, Phil. Mag., 84 (2004), p. 2675.
9. T. Kamino and H. Saka, *Microsc. Microanal. Microstruct.*, 4 (1993), p. 127.
10. H. Mori and H. Yasuda, *Scripta mater.*, 44 (2001), p. 1987.
11. T. Tanaka and S. Hara, *Z. Metallkd.*, 92 (2001), p. 11.
12. T. Tanaka and S. Hara, *Z. Metallkd.*, 92 (2001), p. 467.
13. B.J. Lee, C.S. Oh, and J.H. Shim, *J. Electronic Mater.*, 25 (1996), p. 983.
14. M. Nakamoto et al., Z. Metallkd., 95 (2004), p. 818.
15. J. Lee, W. Shimoda, and T. Tanaka, Mater. Trans., to be published.
16. J. Lee, W. Shimoda, and T. Tanaka, Meas. Sci. Technol., in press.
17. J. Lee, M. Nakamoto, and T. Tanaka, Inter. Sci., in press.
18. T. Iida and R.I.L. Guthrie, *The Physical Properties of Liquid Metals* (Oxford, U.K.: Oxford Science Publications, 1993), p. 71.
19. J.A. Butler, *Proc. Roy. Soc. A.*, 135 (1932), p. 348.
20. K.S. Yeum, R. Speiser, and D.R. Poirier, *Metall. Trans. B.*, 20 (1989), p. 693.
21. T. Tanaka et al., *Z. Metallkd.*, 87 (1996), p. 380.
22. T. Tanaka et al., *Z. Metallkd.*, 89 (1998), p. 368.
23. T. Tanaka et al., *Molten Salt Forum*, 5-6 (1998), p. 213.
24. T. Tanaka, K. Hack, and S. Hara, *MRS Bulletin*, 24 (1999), p. 45.
25. T. Tanaka and S. Hara, *Electrochemistry*, 67 (1999), p. 573.
26. T. Tanaka and S. Hara, *Z. Metallkd.*, 90 (1999), p. 348.
27. T. Ueda, T. Tanaka, and S. Hara, *Z. Metallkd.*, 90 (1999), p. 342.

Junggoo Lee and Hirotaro Mori are with the Research Center for Ultra-High Voltage Electron Microscopy at Osaka University, Japan. Joonho Lee is with the Division of Materials Science and Engineering at Korea University, Korea. Toshihiro Tanaka is with the Department of Materials Process and Engineering at Osaka University, Japan. Karri Penttilä is with the VTT Technical Research Center of Finland.

For more information, contact Junggoo Lee, Research Center for Ultra-High Voltage Electron Microscopy, Osaka University, Yamadaoka 2-1, Suita, Osaka 565-0871, Japan; +81-6-6879-7941; fax +81-6-6879-7942; e-mail; jg-lee@uhvem.osaka-u.ac.jp.